Calorimetric studies of the N-terminal half-molecule of transferrin and mutant forms modified near the Fe^{3+}-binding site

Lung-Nan LIN,* Anne B. MASON,† Robert C. WOODWORTH† and John F. BRANDTS*‡

*Department of Chemistry, University of Massachusetts, Amherst, MA 01003, and †Department of Biochemistry, University of Vermont, Burlington, VT 05405, U.S.A.

The effects of single amino acid substitution on the thermal stability of the N-terminal half-molecule of human transferrin and its iron-binding affinity have been studied by high-sensitivity scanning calorimetry. All site-directed mutations are located on the surface of the binding cleft, and they are D63→S, D63→C, G65→R, H207→E and K206→Q. Differential scanning calorimetry results show that the mutations do not significantly alter the conformational stability of the apo-forms of the proteins. The changes in free energy of unfolding relative to the wild-type protein range from 0.83 to −2.4 kJ/mol. The D63→S, G65→R and H207→E mutations slightly destabilize the apo-protein, while the D63→C and K206→Q mutations increase its stability by a small amount. However, there are large compensating enthalpy–entropy changes caused by all mutations. All mutants bind ferric ion, but with different affinities. Replacement of Asp-63 by either Ser or Cys decreases the apparent binding constant by 5–6 orders of magnitude. The G65→R mutation also decreases the apparent binding constant by 5 orders of magnitude. The K206→*Q* mutation increases the apparent binding constant by 20-fold, while the H207→E mutation does not significantly change the apparent iron-binding affinity of the half-molecule.

INTRODUCTION

The transferrins are a group of iron-transport glycoproteins (approx. 80 kDa) found in the blood plasma and body fluids of many species (Harris and Aisen, 1989; Chasteen and Woodworth, 1990). Each protein is capable of binding two high-spin ferric ions and two synergistic anions. Extensive structural studies (Bailey et al., 1988; Anderson et al., 1989, 1990; Sarra et al., 1990) have revealed that these single-chain proteins are composed of two genetically related lobes (the N- and C-lobes) of about equal size, connected by a short bridging peptide. Each lobe consists of two subdomains, and binds a metal ion and a carbonate or bicarbonate anion. The binding site is located in the deep cleft between the two subdomains. Early physical chemical studies (Aisen et al., 1978; Brock, 1985) established that the binding properties of the C- and N-lobes are similar, but not identical. Recent studies on human serum transferrin (hTF) and the egg white protein known as ovotransferrin, using titration calorimetry (Lin et al., 1991; L.-N. Lin, A. B. Mason, R. C. Woodworth and J. F. Brandts, unpublished work), have shown not only that the binding properties of the C- and N-sites are energetically and kinetically different, but also that both sites of hTF are quite different from those of ovotransferrin.

To gain further insight into the structure and the binding properties of transferrins, a recombinant form of the wild-type N-terminal half-molecule of hTF (hTF/2N) and five site-directed mutants have been expressed in baby hamster kidney cells and purified to homogeneity (Funk et al., 1990; Woodworth et al., 1991). The half-molecule comprises residues 1–337 and terminates within the bridging peptide, considered to be residues 332–338. Each of the amino acid substitutions in the mutants is located on the surface within the binding cleft. Asp-63, which is one of four amino acid side chains bound to the ferric ion, has been replaced by either serine or cysteine. Asp-63→Ser (D63→S) is a naturally occurring mutation found in the C-terminal lobe of melanotransferrin (Rose et al., 1986). It has been speculated that Ser-63 abrogates normal iron binding (Chasteen and Woodworth, 1990). Gly-65, just two residues away and near the binding site, has been replaced by arginine (G65→R) to examine the effect of a positively charged side chain on the binding affinity (Woodworth et al., 1991). Two amino acid residues which are located in the hinge region of the binding cleft, Lys-206 and His-207, have been mutated to glutamine and glutamic acid respectively. The K206→Q mutation occurs naturally in the C-terminal lobe of ovotransferrin, which has been reported to bind ferric ion two orders of magnitude more tightly than the N-terminal lobe (Ulundu, 1989). The H207→E mutation is found in the N-terminal lobe of human lactoferrin, which binds iron more tightly than does serum transferrin (Harris, 1989).

A preliminary characterization of binding affinity for ferric ion for the wild-type hTF/2N and these five mutants has been reported (Woodworth et al., 1991). In the present paper, an ultrasensitive differential scanning calorimetry (d.s.c.) technique was employed to study the effects of the single amino acid substitutions on the structure and iron-binding affinity of the half-molecule. Our results show that Asp-63 is critical for the tight binding of iron. The replacement of Asp-63 by either serine or cysteine causes an apparent decrease in binding affinity of approx. 5–6 orders of magnitude. Our data also show that introducing a positive charge near the binding site decreases the binding affinity by approx. 5 orders of magnitude. In agreement with previous observations for lactoferrin and ovotransferrin, the K206→Q and H207→E mutations enhance iron binding. The d.s.c. data also show that, in spite of the large differences in binding affinity, the apparent stabilities of the apo-forms of the mutant proteins are very similar. However there are large compensating enthalpy–entropy changes caused by all mutations.

Abbreviations used: hTF, human serum transferrin; hTF/2N, recombinant N-terminal half-molecule of human transferrin, ending at Asp-337; NTA, nitrilotriacetate; d.s.c., differential scanning calorimetry; $\Delta H_{cal.}$, calorimetric heat; ΔH_{VH}, van't Hoff heat; ΔC_p, heat capacity change; $\Delta(\Delta G^\circ)$, apparent stability of mutant compared with wild type.

‡ To whom correspondence should be addressed.

MATERIALS AND METHODS

Materials

hTF/2N and five of its site-directed mutants (D63→S, D63→C, G65→R, K206→Q and H207→E) were used in the present d.s.c. study. The expression, purification and initial characterization of these proteins have been described in detail (Funk et al., 1990; Woodworth et al., 1991). All hTF/2N samples were purified in the holo-form. The wild-type and all mutants showed only a single peak on Polyanion SI columns (Pharmacia). The apo-forms of proteins were obtained by removing iron from the proteins with 0.5 M acetate, 1 mM EDTA and 1 mM nitrilotriacetate (NTA), pH 5.0, using Centricon microconcentrators (Amicon). With one exception, d.s.c. results indicated nearly 100% capability of binding ferric ion, as shown by the complete disappearance of the transition of the apo-form at low transition temperature (T_m) and conversion to the transition of the holo-form at high T_m when saturating amounts of ferric ion were added. The single exception was the D63→C mutant preparation, where approx. 15% of the transition area indicative of the apo-form could not be shifted by adding saturating amounts of ferric ion, suggesting the presence of a modified form of the protein incapable of binding iron. Mass analysis of the D63→C preparation was consistent with cysteinylation of D63→C (Woodworth et al., 1991); the nature of the impurity is unknown.

Since the chromatographic purity of the preparations and their complete convertibility from the apo- to the holo-form (with the exception of D63→C) was established, we elected to determine the molar concentrations of the apo-proteins by their quantitative ability to bind ferric ion using ultrasensitive titration calorimetry (Lin et al., 1991). This was carried out for the wild-type hTF/2N as well as for its mutants. We found that a 1:1 stoichiometry (within ±5%) was obtained by assuming a molar absorption coefficient of 40000 $M^{-1} \cdot cm^{-1}$ at 278 nm. This value is consistent with that (40000 ± 500 $M^{-1} \cdot cm^{-1}$) from the amino acid composition of hTF/2N, as determined by the method of Gill and von Hippel (1989), and approx. 3–4% higher than previously reported (Funk et al., 1990; Woodworth et al., 1991). Here the molar absorption coefficient of 40000 $M^{-1} \cdot cm^{-1}$ was used to determine the concentrations of all apo-forms of the half-molecules, since it was consistent with a 1:1 stoichiometry for the wild-type and mutants, except for D63→C, where ferric ion binding was too low by 20%. The concentrations of the holo-forms were determined from the visible spectra as described previously (Woodworth et al., 1991).

D.s.c. measurements

The d.s.c. experiments were carried out on a MicroCal MC-2 ultrasensitive microcalorimeter (MicroCal Inc., Northampton, MA, U.S.A.), interfaced with a 386 personal computer. A Windows-based software package (Origin), also supplied by MicroCal, was used for data analysis and plotting. The instrumentation and experimental procedures for d.s.c. have been described in detail elsewhere (Brandts et al., 1989; Bailey et al., 1990; Brandts and Lin, 1990). All d.s.c. measurements were carried out in 0.5 M Hepes and 25 mM $NaHCO_3$, pH 7.5.

RESULTS

D.s.c. data for the apo-form of the recombinant wild-type hTF/2N and five of its site-directed mutants are shown in Figure 1. A scan on native, intact hTF is also shown, where the transition with highest T_m (near 69 °C) is due to unfolding of the N-lobe. The d.s.c. scan rate was approx. 81.5 °C/h for all experiments, and protein concentrations were 1–2 mg/ml. Initially, d.s.c. experiments were carried out in 0.1 M Hepes and 25 mM $NaHCO_3$, pH 7.5, but the thermal reversibility of proteins was found to be low. However, in 0.5 M Hepes and 25 mM $NaHCO_3$, pH 7.5, reversibility was substantially improved, so all data presented were obtained using the latter buffer. The d.s.c. traces shown in Figure 1 were also corrected for the instrument baseline (i.e. buffer versus buffer run) and normalized with regard to protein concentration. A second scan was also carried out for each protein immediately following the first scan to check the extent of the thermal reversibility. The results of the second scan (not shown) indicate that the thermal reversibility for the apo-proteins is more than 80% for the wild type and approx. 60–70% for mutants when the first heating is stopped at a temperature immediately after the end of the transition. The high reversibility for the apo-proteins suggests that the thermal traces in Figure 1 are not significantly distorted by irreversible effects.

Transitions for apo-hTF/2N molecules could not generally be fitted satisfactorily by assuming a single two-state transition, so the method illustrated in Figure 2 for the wild-type fragment was used for estimating transition parameters for all forms. Based on linear high- and low-temperature baselines (broken lines), the progress baseline in the transition region (solid line) was determined using an iterative algorithm in MicroCal's instrument software. [This algorithm forms the progress baseline such that,

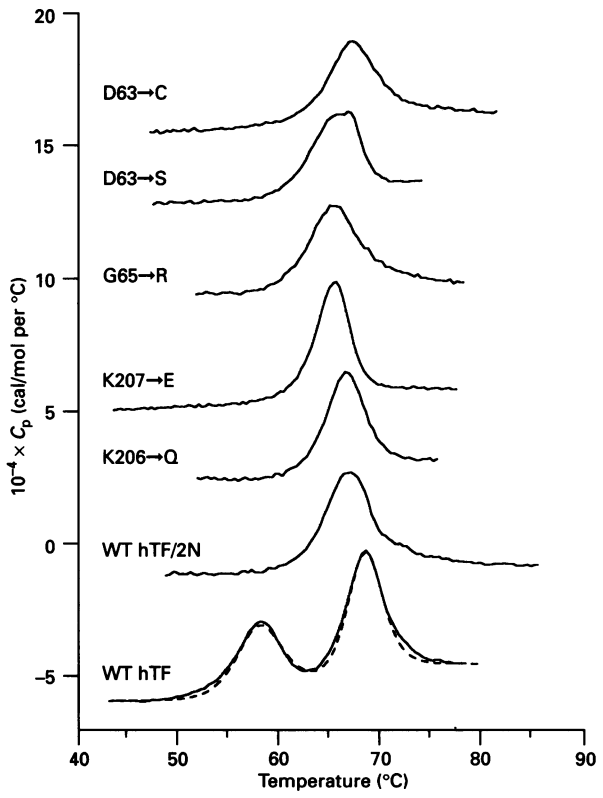

Figure 1 D.s.c. scans of apo-forms of the recombinant wild-type (WT) hTF/2N and its site-directed mutants, and of native hTF

The broken line results from fitting the data on native hTF to two two-state transitions. Protein concentrations were 1–2 mg/ml. All experiments were carried out in 0.5 M Hepes and 25 mM $NaHCO_3$, pH 7.5. Scan rates were 81.5 °C/h. For clarity, d.s.c. traces have been arbitrarily shifted on the ordinate scale. Note that 1 cal = 4.184 J.

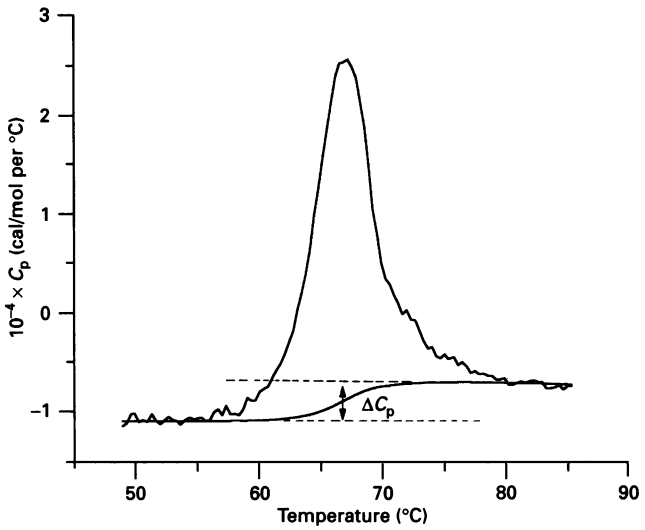

Figure 2 The integration area method for obtaining the thermal transition parameters

First, the high- and low-temperature baselines were linearly extended (broken lines). Then, the progress baseline in the transition region was formed (solid line). The ΔH was determined as the area between the experimental data and the progress baseline. The T_m was taken as the temperature where one-half of the total area had been generated. ΔC_p was obtained at T_m, as indicated in the Figure. 1 cal = 4.184 J.

Table 1 Thermodynamic parameters obtained from d.s.c. for the apo-form of the recombinant wild-type hTF/2N and five of its site-direct mutants, and the N-lobe of the native hTF

Estimated uncertainties: $\Delta H_{cal.}$, ±50 kJ/mol; T_m, ±0.5 °C; ΔC_p, ±5 kJ/mol per °C; $\Delta(\Delta G^\circ)$, ±0.1 kJ/mol.

Protein	$\Delta H_{cal.}$ (kJ/mol)	ΔH_{VH} (kJ/mol)	T_m (°C)	ΔC_p (kJ/mol per °C)	$\Delta(\Delta G^\circ)$ (kJ/mol)
Wild type	927	590	66.4	20	0
D63→S	690	644	65.6	16	−1.6
D63→C	715	582	66.8	28	0.83
G65→R	720	552	65.3	16	−2.4
H207→E	750	858	65.6	19	−1.8
K206→Q	720	749	66.5	28	0.21
N-lobe (hTF)	983	858	68.35	30	5.4

at any temperature in the transition region, the distance from the extrapolated low-temperature baseline to the progress baseline divided by the total distance between low- and high-temperature baselines at the same temperature is equal to the fractional area (i.e. between the experimental data and the progress baseline) that has been formed up to that temperature relative to the total area in the transition. For a two-state transition, the progress baseline would correspond to the static partial molar heat capacity of the mixture of the two states that exists at the temperature.] The calorimetric heat, $\Delta H_{cal.}$, was determined as the total area between the experimental data and the progress baseline, while T_m was taken as the temperature at which one-half of the total area had been generated. These parameters are given in Table 1 for each apo-form. The van't Hoff heat, ΔH_{VH}, was determined for each scan by first subtracting the progress baseline to remove the heat capacity effect and then curve-fitting to a non-two-state model. These values are also shown in Table 1. The calorimetric heats obtained from the curve-fitting (not shown) to a non-two-state model were similar to those obtained from area measurements, but less reliable, since the fits were not exact.

In contrast to a $\Delta H_{cal.}$ of 927 kJ for the wild type, the mutants all show reduced values of approx. 700–750 kJ. With the exception of H207→E and K206→Q, the mutants and the wild type have a ΔH_{VH} which is smaller than the $\Delta H_{cal.}$. The ratio $\Delta H_{cal.}/\Delta H_{VH}$ ranges from 0.87 for H207→E to 1.57 for the wild type. The fact that the ratio is somewhat larger than unity for most forms suggests that multiple transitions occur within a single peak and that the transitions are less than 100% coupled. The same situation is seen for the transition of the N-lobe in intact hTF (Table 1), where the $\Delta H_{cal.}$ is more than 100 kJ larger than the ΔH_{VH}. It is known that each lobe in transferrins is composed of two subdomains (Anderson et al., 1989, 1990; Bailey et al., 1988), each forming part of the binding cleft, and this structural feature might well contribute to the transition broadening which causes deviations from two-state behaviour for most forms.

Values for the heat capacity change (ΔC_p) of unfolding are also shown in Table 1, and range from 16 to 30 kJ/mol per °C. These estimates are uncertain, due to the usual difficulty of extrapolating high- and low-temperature baselines and to the additional complication which is introduced by irreversible effects at high temperature.

On comparing the wild-type apo-hTF/2N with the corresponding transition of the N-lobe in intact apo-hTF (Figure 1) in more detail, it is seen in Table 1 that the T_m for the half-molecule (66.4 °C) is significantly lower than for the N-lobe in the intact hTF (68.35 °C). Since the transition for the N-lobe in the intact molecule is much higher than for the C-lobe, it appears possible that the N-lobe is stabilized in the intact molecule by interaction with the unfolded C-lobe. An alternative explanation is that genetic termination of the N-fragment at residue 337, considered to be in the bridging peptide connecting the N- and C-lobes, eliminates or modifies some interactions which are important to the stability of the folded N-lobe. In spite of the small difference in stability, the ΔH values are almost identical at their respective T_m values. Another notable difference is the fact that the N-lobe of the intact hTF conforms to the two-state model much more closely ($\Delta H_{cal.}/\Delta H_{VH}$ ratio of 1.15) than does the wild-type fragment (ratio of 1.57). The fit of the scan on intact hTF to two two-state transitions is shown as the broken line in Figure 1.

In contrast to the differences in heats of transition, there are only small differences in T_m values between mutants and wild-type apo-proteins, ranging from a few tenths of a degree higher (D63→C and K206→Q) to about a degree lower (D63→S, G65→R, and H207→E). From the shift in T_m, the changes in the apparent stability of the mutants relative to the wild-type (WT), $\Delta(\Delta G^\circ)$, can be evaluated at the T_m of the wild-type hTF/2N by the following equation:

$$\Delta(\Delta G^\circ) = \Delta G^\circ(\text{mutant}) - \Delta G^\circ(\text{WT})$$

ΔG°(WT) is zero at T_m, while the ΔG°(mutant) can be obtained by the following form of the Gibbs–Helmholtz equation:

$$\Delta G^\circ(\text{mutant}) =$$

$$\Delta H\left(1-\frac{T_m}{T_m'}\right)-\Delta C_p\left(T_m'-T_m+T_m\cdot\ln\frac{T_m}{T_m'}\right)$$

where T_m and T_m' are the transition temperature for wild-type and mutant respectively, ΔH is the calorimetric enthalpy of the

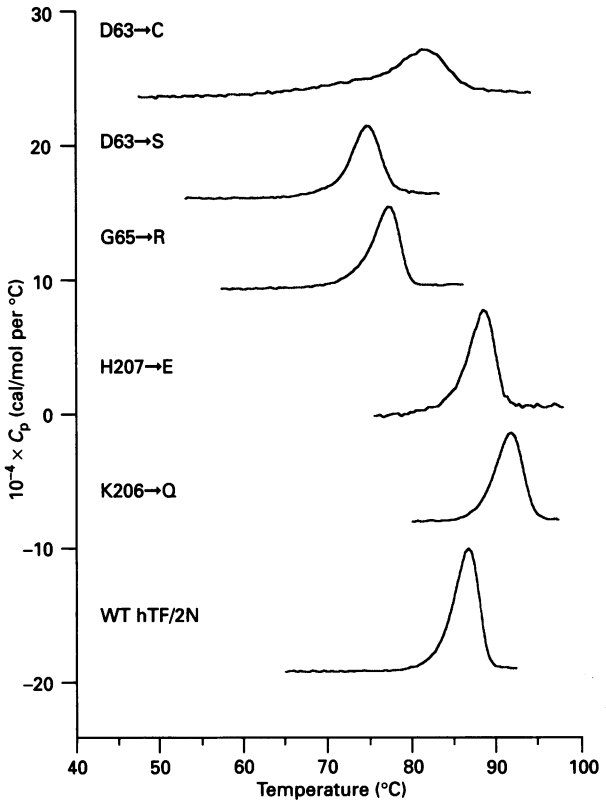

Figure 3 D.s.c. scans on holo-forms of the recombinant wild-type (WT) hTF/2N and its site-directed mutants

The experimental conditions are the same as those in Figure 1. D.s.c. traces have been arbitrarily shifted on the ordinate scale. 1 cal = 4.184 J

Table 2 Thermodynamic parameters obtained from d.s.c. for the holo-form of wild-type hTF/2N and five of its site-directed mutants

Estimated uncertainties: $\Delta H_{cal.}$, ±50 kJ/mol; T_m and ΔT_m, ±0.5 °C; ΔC_p, ±5 kJ/mol per °C.

Protein	$\Delta H_{cal.}$ (kJ/mol)	T_m (°C)	ΔC_p (kJ/mol per °C)	ΔT_m (°C)
Wild type	1477	86.0	17	19.6
D63→S	1038	74.3	18	8.7
D63→C	1146	80.8	–	14.0
G65→R	1100	76.7	13	11.4
H207→E	1305	87.7	25	22.1
K206→Q	1205	90.9	13	24.4

mutant at T_m', and ΔC_p is the heat capacity change for the mutant. The values of $\Delta(\Delta G^\circ)$ are listed in Table 1. They are relatively small, ranging from decreased stability of approx. 2.4 kJ for G65→R to an increased stability of 1 kJ for D63→C. As will be seen, these small changes in stability of the apo-forms of the mutants are in marked contrast to the situation existing for the holo-forms.

Transitions for the holo-forms are shown in Figure 3. Second scans indicated somewhat lower reversibility than for apo-forms, i.e. approx. 50–60%, resulting perhaps from their much higher T_m values. The transitions show an extremely poor fit to a single two-state model, much worse in all cases than for the equivalent apo-form. This is to be expected, since at low temperature there was essentially no unbound ferric ion (i.e. all excess Fe-NTA was dialysed away before doing d.s.c. experiments), so the rapid increase in unbound ferric ion as a function of the degree of unfolding would be expected to substantially broaden the transitions for the holo-forms and skew them toward the low-temperature side. This type of ligand-broadening effect can be readily demonstrated in mathematical simulations using two-state models. Transition parameters for the holo-forms (Table 2) were determined in the same way as for the apo-forms. Because of the broadening effect from released ferric ions, curve-fitting to obtain ΔH_{VH} values was not carried out on the holo-proteins.

Transition parameters are summarized in Table 2. Two of the mutants, H207→E and K206→Q, show a higher T_m (87.7 and 90.9 °C respectively) than that of the wild type (86.0 °C), while mutants D63→S, G65→R and D63→C have lower T_m values of 74.3, 76.7 and 80.8 °C respectively. Differences in T_m values between corresponding holo- and apo-forms vary from 8.7 to 24.4 °C for the mutants, compared with 19.6 °C for the wild type. The values of ΔH for the various mutant holo-forms, 1038–1305 kJ, are substantially lower than for the wild-type (1477 kJ), as was also noted earlier with respect to the apo-forms. ΔC_p values are 13–25 kJ/mol per °C which are similar to those of the apo-forms. If T_m shifts are used to estimate the affinity of iron binding, the order of increasing affinity is as follows: D63→S < G65→R < D63→C ≪ wild type < H207→E < K206→Q. These data are in excellent agreement with a preliminary characterization of the relative iron-binding affinities of the wild-type N-terminal half-molecule and these same mutants using urea gel electrophoresis (Woodworth et al., 1991).

It has been shown (Brandts et al., 1989; Brandts and Lin, 1990) that apparent binding constants can be quantitatively evaluated from the ligand-induced T_m shift and the calorimetric parameters (i.e. T_m, ΔH and ΔC_p) for reversible transitions. [Equations derived in Brandts and Lin (1990) to obtain binding constants from d.s.c. data were derived with an assumption of two-state transitions, and this assumption does not strictly apply to the data under consideration here. If the same equations are to be applied to non-two-state transitions, then the $\Delta H_{cal.}$, and not the ΔH_{VH}, must be used in the calculations, since this represents the true difference in molar enthalpy between the low-temperature native state and the final high-temperature unfolded state. An additional assumption is implicit when using the derived two-state equations for non-two-state transitions, and this assumption involves the relative free energies of the initial and final states at transition midpoints T_m. If the two-state equations are to be strictly valid for non-two-state transitions, then the initial and final states must have the same difference in free energy at T_m in the absence of ligand as they do at the higher T_m in the presence of ligand. This free energy difference need not be zero, as it is for two-state transitions, but merely constant.] Here, the equation for numerical calculation can be expressed as:

$$K_L(T_m) = \frac{\left\{\exp.\left[\frac{-\Delta H(T_o)}{R}\left(\frac{1}{T_m}-\frac{1}{T_o}\right)+\frac{\Delta C_p}{R}\left(\ln\frac{T_m}{T_o}+\frac{T_o}{T_m}-1\right)\right]\right\}}{[L]_{T_m}}$$

where T_o and T_m are midpoint for transition before and after binding of ligand, $\Delta H(T_o)$ is the enthalpy change of the apo-form at T_o, ΔC_p is the heat capacity change for the transition, and $[L]_{T_m}$ is free ligand concentration at T_m.

Although T_m values were measured with high precision, the

ΔH and ΔC_p values in Tables 1 and 2 are subject to large uncertainties. The most reliable calorimetric data in Tables 1 and 2 are those for the apo-form of the wild type, and these were used to estimate semi-quantitatively the apparent binding constant at the T_m for the holo-form. The data needed for this calculation are the T_m values of the apo- and holo-forms and the ΔH and ΔC_p values of the apo-form. An apparent binding constant of approx. 5×10^{13} M^{-1} was obtained for the wild-type N-terminal half-molecule at 86 °C, which is identical to the value estimated for the N-site of intact hTF at 88 °C (L.-N. Lin, A. B. Mason, R. C. Woodworth and J. F. Brandts, unpublished work). The error in these estimates might be as high as a factor of 10, due to the possible errors in ΔH and ΔC_p. If the T_m shifts and calorimetric parameters for the D63→S mutant listed in Tables 1 and 2 are used to evaluate the apparent binding constant for mutant D63→S, a value of approx. 3×10^7 would be obtained, which is around six orders of magnitude smaller than that of the wild type. This emphasizes the importance of Asp-63 for the tight binding of iron. Using the same calculation, the K206→Q mutant has an apparent binding constant which is about 20 times higher than that of the wild type and about the same as that of the H207→E mutant. The apparent binding constant for G65→R is around five orders of magnitude smaller than that of the wild type, indicating that introducing a positive charge near the binding site greatly reduces the affinity for ferric ions.

DISCUSSION

The d.s.c. data presented here on apo-hTF, as well as more extensive data (L.-N. Lin, A. B. Mason, R. C. Woodworth and J. F. Brandts, unpublished work), show that each of the N- and C-lobes of the whole molecule behaves nearly as a single co-operative unit during thermal unfolding, even though X-ray crystallography clearly shows that both the N- and C-lobes consist of two distinct subdomains. The transitions of the two subdomains in each lobe of the whole molecule presumably are almost completely coupled energetically during the thermal unfolding, as indicated in this study by a $\Delta H_{cal.}/\Delta H_{vH}$ ratio of 1.15 for the N-lobe in the intact hTF. Our d.s.c. data on the apo-forms of hTF/2N also show only a single transition peak. However, the transitions of the two subdomains in the half-molecule are apparently less strongly coupled than in the intact molecule, as indicated by a higher $\Delta H_{cal.}/\Delta H_{vH}$ ratio of 1.57. Also, the T_m of the wild-type half-molecule is approx. 2 °C lower than that of the N-lobe in the intact hTF. Since the N-lobe has the higher T_m in the intact molecule, the lower T_m for the half-molecule might suggest that the absence of the 'unfolded' C-lobe slightly destabilizes the folded N-half-molecule. It seems possible that some of the residues located in the genetically defined C-lobe could actually participate in the folded structure of the N-lobe in the intact molecule. Indeed, the X-ray structure reveals that the C-terminal peptide of the C-lobe interacts with the C-terminal peptide of the N-lobe, in which case its absence in the N-half-molecule might result in destabilization. There are some indications of differences between the N-terminal half-molecule of lactoferrin relative to holo-lactoferrin, where iron release was found to occur at a higher pH in both proteolytically derived (Legrand et al., 1990) and recombinant (Day et al., 1992) lactoferrin/2N. However, no such differences were noted in iron release from the proteolytically derived N-terminal half-molecule of human serum transferrin (Lineback-Zins and Brew, 1980) relative to holo-transferrin.

The mutations have only a minor effect on the conformational stability of the apo-hTF/2N molecule. The D63→S, G65→R and H207→E mutations slightly destabilize the apo-protein, but changes in $\Delta(\Delta G^o)$ values are smaller in magnitude than 2.5 kJ/mol. The K206→Q and D63→C mutations increase conformational stability by a small amount. Since all mutation sites are located in the cleft between subdomains of the protein, and since the side-chains appear not to be buried, the free energy changes caused by mutations most likely reflect minor changes in the interaction between subdomains of the half-molecules.

In general, the mutations caused a decrease of approx. 200 kJ in calorimetric $\Delta H_{cal.}$ for the thermal transition without a corresponding change in ΔG^o, which means that there is also a large decrease in entropy. A lack of correlation between changes in free energies and enthalpies of thermal unfolding caused by mutations has been observed for phage T4 lysozyme (Hawkes et al., 1984; Connelly et al., 1991), P22 tailspike protein (Sturtevant et al., 1989), Staphylococcal nuclease (Shortle et al., 1988) and λ repressor (Hecht et al., 1984). Hawkes et al. (1984), in their study of T4 lysozyme, suggested that the compensating enthalpy/entropy changes can be attributed to either (1) enhanced fluctuations in the mutant native state, perhaps through the formation of a partially unfolded loop, or (2) distortion of local geometry in the native state that results in an increase in strain enthalpy and a higher vibrational entropy. More recently, Shortle et al. (1988) proposed that the enthalpy/entropy compensation is the consequence of large changes in the solvation of the denatured state that result from the amino acid replacement. However, this explanation seems less likely to us.

D.s.c. data on the holo-proteins show the importance of Asp-63 for the tight binding of ferric ion. The replacement of the negatively charged Asp-63 by serine or cysteine decreases the apparent binding constant by approx. 5–6 orders of magnitude. Data on the G65→R mutant suggest that a positive charge near the binding site also greatly reduces the binding affinity for ferric ion. Two of the mutations which were studied here, K206→Q and H207→E, are analogous to natural differences existing between hTF and other transferrins. Both were found to enhance the binding affinity for iron, in contrast to the other mutations which substantially decreased affinity. These two amino acid residues are located at the hinge region of the binding cleft between the two subdomains. Each mutation increases the formal negative charge of protein by 1, indicating that an increased negative charge in the binding pocket favours iron binding.

This study was supported by grants from the National Institutes of Health to J.F.B. (GM-42636) and to R.C.W. (DK-21739).

REFERENCES

Aisen, P., Leibman, A. and Zweier, J. (1978) J. Biol. Chem. **253**, 1930–1937
Anderson, B. F., Baker, H. M., Norris, G. E., Rice, D. W. and Baker, E. N. (1989) J. Mol. Biol. **209**, 711–734
Anderson, B. F., Baker, H. M., Norris, G. E., Rumball, S. V. and Baker, E. N. (1990) Nature (London) **344**, 784–787
Bailey, S., Evans, R. W., Garrat, R. C., Gorinsky, B., Hasnaint, S., Horsburgh, C., Jhoti, H., Lindley, P. F., Mydin, A., Sarra, R. and Watson, J. L. (1988) Biochemistry **27**, 5804–5812
Bailey, J. M., Lin, L.-N., Brandts, J. F., and Mas, M. T. (1990) J. Protein Chem. **9**, 59–67
Brandts, J. F. and Lin, L.-N. (1990) Biochemistry **29**, 6927–6940
Brandts, J. F., Hu, C. Q., Lin, L.-N. and Mas, M. T. (1989) Biochemistry **28**, 8588–8596
Brock, J. (1985) in Metalloproteins (Harrison, P. M., ed.), part 2, pp. 183–262, Verlag Chemie, Weinheim
Chasteen, N. D. and Woodworth, R. C. (1990) in Iron Transport and Storage (Ponka, P., Schulman, H. M. and Woodworth, R. C., eds.), pp. 68–79, CRC Press, Boca Raton, FL
Connelly, P., Ghosaini, L., Hu, C. Q., Kitamura, S., Tanaka, A. and Sturtevant, J. M. (1991) Biochemistry **30**, 1887–1891
Day, C. L., Stowell, K. M., Baker, E. N. and Tweedie, J. W. (1992) J. Biol. Chem. **267**, 13857–13862
Funk, W. D., MacGillivray, R. T. A., Mason, A. B., Brown, S. A. and Woodworth, R. C. (1990) Biochemistry **29**, 1654–1660

Gill, S. C. and von Hippel, P. H. (1989) Anal. Biochem. **182**, 319–326
Harris, D. C. and Aisen, P. (1989) in Iron Carrier and Iron Proteins (Loehr, T. M., ed.), pp. 239–351, VCH Publishers, New York
Harris, W. R. (1989) Adv. Exp. Med. Biol. **249**, 67–93
Hawkes, R., Grutter, M. G. and Schellman, J. (1984) J. Mol. Biol. **175**, 195–212
Hecht, M. H., Sturtevant, J. M. and Sauer, R. T. (1984) Proc. Natl. Acad. Sci. U.S.A. **81**, 5685–5689
Legrand, D., Mazurier, J., Colavizza, D., Montreuil, J. and Spik, G. (1990) Biochem. J. **266**, 575–581
Lin, L.-N., Mason, A. B., Woodworth, R. C. and Brandts, J. F. (1991) Biochemistry **30**, 11660–11669

Received 27 October 1992/12 February 1993; accepted 11 March 1993

Lineback-Zins, J. and Brew, K. (1980) J. Biol. Chem. **255**, 708–713
Rose, T. M., Plowman, G. D., Teplow, D. P., Dreyer, W. J., Hellstrom, K. E. and Brown, T. P. (1986) Proc. Natl. Acad. Sci. U.S.A. **83**, 1261–1265
Sarra, R., Garratt, R., Gorinsky, B., Jhoti, H. and Lindley, P. (1990) Acta Crystallogr. Sect. B **B46**, 763–771
Shortle, D., Meeker, A. K. and Freire, E. (1988) Biochemistry **27**, 4761–4768
Sturtevant, J. M., Yu, M.-h., Hasse-Pettingill, C. and King, J. (1989) J. Biol. Chem. **264**, 10693–10698
Ulundu, L. S. (1989) Ph.D. Thesis, University of Vermont, Burlington, VT
Woodworth, R. C., Mason, A. B., Funk, W. D. and MacGillvray, R. T. A. (1991) Biochemistry **30**, 10824–10829